Journal of Marine Science and Technology

Volume 28 | Issue 3 Article 1

NONLINEAR BREAKING-WAVE CHARACTERISTICS IN LAGRANGIAN COORDINATES

Wen-Jer Tseng
Department of Civil Engineering and Geomatics, Cheng Shiu University

Chia-Yan Cheng
Taiwan Ocean Research Institute, National Applied Research Laboratories

Journal of Marine Science and Technology, Vol. 28, No. 3, pp. 149-157 (2020)
DOI: 10.6119/JMST.202006_28(3).0001

NONLINEAR BREAKING-WAVE CHARACTERISTICS IN LAGRANGIAN COORDINATES

Wen-Jer Tseng[1] and Chia-Yan Cheng[2]

Key words: Eulerian system, Lagrangian system, breaking-wave characteristics.

ABSTRACT

This paper presents a theoretical investigation of nonlinear surface-wave propagation over a sloping bottom. For a problem with nonlinear surface-wave propagation over a sloping bottom, a perturbation method is first used to find the analytical solution in order to derive the third order terms for the bottom slope α and the wave steepness ε in the Eulerian system. Then, by transforming the flow field solution from the Eulerian system into the Lagrangian system, a more accurate wave profile is identified. By using the kinematic stability parameter, new theoretical breaking-wave characteristics are derived. The theoretical solutions are then compared with those from other research. The results reveal that the present solution reasonably describes the wave-breaking phenomenon. In this paper, a new theoretical solution for the breaking-wave characteristics is provided, and it is a useful approach for predicting breaking-wave characteristics.

I. INTRODUCTION

Because of changes in water depth, a wave touches the bottom when the depth is shorter than half of its wavelength, and the wave shoals when travelling from deep water to shallow water. The wave height increases, and the wave profile becomes more skewed and asymmetric (Elgar and Guza, 1985) owing to the nonlinear effects. The celerity is reduced; hence, the fluid particle velocity of the wave crest is faster than the celerity, and the wave breaks. A breaking wave releases enormous energy and substantial impact force, which damages coastal structures such as breakwaters and causes sediment transport along and across nearby shores. Therefore, breaking-wave characteristics must be quantified to obtain reliable predictions about sediment transport and structural design in coastal regions. Most investigators have discussed and inducted formulae from experimental studies. For example, Street and Camfield (1966), Tang (1966), L'e M'ehaut'e and Koh (1967), Galvin (1968), Goda (1970, 2004), Saeki et al. (1971), Sunamura and Horikawa (1974), Sunamura (1980, 1983), Ogwa and Shuto (1984), Seyama and Kimura (1988), Hansen (1990), and Rattanapitikon and Shibayama (2000) have all proposed empirical formulae or semiempirical formulae for breaking-wave height and breaking-wave depth as a function of deep-water wave height, wave steepness, and bottom slope, in accordance with experiments or reliable field data. Chang (1999), Gotoh and Sakai (1999), and Hsieh et al. (2007, 2008) have studied breaking-wave characteristics by means of numerical simulation, and Deo et al. (2003) studied the same topic by means of neural networks and experimental results. Iwagaki et al. (1974), Chanson and Lee (1997), Ting et al. (2002), Tsai et al. (2005), and Hsiao et al. (2008) have used experimental data to examine some empirical formulae and characteristics related to breaking waves. The major drawback for all of the aforementioned studies has been that they could only derive the breaking-wave height or breaking-wave depth and the location of a wave when breaking; however, these studies have not been able to completely describe the process of the wave deformation and of the related flow field.

Biesel (1952) suggested a plausible approximation method to account for normal incident waves propagating on a sloping bottom, with the bottom slope taken into account in the velocity potential as a perturbation parameter, but wave breaking and nonlinear effects are not addressed in that study. Furthermore, Biesel did not explain the derivation of the formula in detail. Keller (1958), Chen and Tang (1992), Hsu et al. (2001), and Chen et al. (2005, 2006) have extended Biesel's theory.

In this study, a nonlinear analysis was undertaken by perturbing to the third order of the bottom slope α or the wave steepness ε in an Eulerian system. Then, the profile of the breaking wave was determined using a transformation into a Lagrangian system. The breaking-wave height and the breaking wave depth can be derived using kinematic stability

Paper submitted 10/23/18; revised 12/03/18; accepted 03/15/19. Corresponding Author: Chia-Yan Cheng(E-Mail: cycheng@narlabs.org.tw)
[1] Department of Civil Engineering and Geomatics, Cheng Shiu University
[2]Taiwan Ocean Research Institute, National Applied Research Laboratories

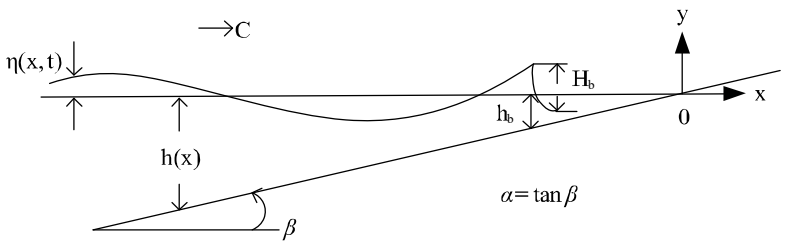

Fig. l. Sketch definition for a surface wave propagating on a gently sloping bottom.

parameters. Finally, the theoretical solutions were verified by comparing them with those from other studies, as shown in Fig. 3 to Fig. 5.

II. MATHEMATICAL FORMULATION

To describe a surface wave propagating toward a gently and uniformly sloping bottom, a two-dimensional Cartesian $x-y$ coordinate system is used, as shown in Fig. l. The negative *x*-axis is directed outward to the sea, and the positive *y*-axis extends vertically upward from the still water level; the bottom, or the seabed, is at $y = -h = \alpha x$, where α denotes the bottom slope (Li et al., 2013).

In Fig. 1, angle β is the incline of the bottom, α (= tan β) is the bottom slope, $\eta(x,t)$ is the elevation of the water's surface, C is celerity, $h(x)$ is water depth, H_b is breaking-wave height, and h_b is breaking-wave depth.

Assume that the flow field is irrotational, incompressible, and inviscid. The governing equations and boundary conditions can be derived to the third order of the bottom slope α or of the wave steepness $\varepsilon (= H_o / L_o)$, where H_o is the wave height and L_o is the wavelength of a deep-water wave or an incident wave. To describe the irrotational motion of an inviscid and incompressible fluid, a velocity potential $\phi(x, y, t)$ is introduced, and the horizontal and vertical velocities are given by

$$u = \frac{\partial \phi}{\partial x},\ v = \frac{\partial \phi}{\partial y},\ \vec{V} = u\vec{i} + v\vec{j}. \tag{1}$$

The velocity potential $\phi(x, y, t)$ is harmonic with respect to *x* and *y* and satisfies the continuity equation. This leads to the Laplace equation

$$\nabla^2\phi = \frac{\partial^2\phi}{\partial x^2} + \frac{\partial^2\phi}{\partial y^2} = 0 \tag{2}$$

The wave motion described must satisfy boundary conditions at the bottom and at the free surface, respectively, as follows:

1. On an immovable and impermeable sloping bottom with an incline β to the horizon, the bathymetry is represented by $f(x,y) = y + h = y - \alpha x = 0$, and the no-flux bottom boundary condition gives

$$\nabla\phi \cdot \vec{n} = \nabla\phi \cdot \frac{\nabla f}{|\nabla f|} = \frac{-\alpha\phi_x + \phi_y}{\sqrt{1+\alpha^2}} = 0,\ y = -h,\ \alpha > 0 \text{ and } x \le 0\ ,$$

or simply

$$\frac{\partial \phi}{\partial y} - \alpha\frac{\partial \phi}{\partial x} = 0,\ y = -h\ . \tag{3}$$

2. The dynamic and kinematic free-surface boundary conditions are

$$\phi_t + (\nabla\phi)^2/2 + g\eta = 0,\ y = \eta \tag{4}$$

$$\phi_y = d\eta/dt\ ,\ y = \eta \tag{5}$$

Taking the total differential D/Dt of Equation (4) and using Equation (5) gives

$$\phi_{tt} + g\phi_y + [(\nabla\phi)^2]_t + \nabla\phi\cdot\nabla(\nabla\phi)^2/2 = 0,\ y = \eta \tag{6}$$

3. A time-averaged mass flux conservation condition is required: The water mass bounded by the shoreline created by the sloping bottom rushes up and down the beach face, and the total mass does not change. Therefore, at any cross-section where x is a constant, the time-averaged mass flux should vanish. This condition gives

$$\begin{aligned} &y-direction:\ \frac{1}{T}\int_0^T\int_{-h}^{\eta}\phi_y\,dydt = \\ &\overline{\int_{-h}^{\eta}\phi_y\,dy} = \overline{(\phi)_{y=\eta}} - \overline{(\phi)_{y=-h}} = 0, \end{aligned} \tag{7}$$

$$\begin{aligned} &x-direction:\ \frac{1}{T}\int_0^T\int_{-h}^{\eta}\phi_x\,dydt - \frac{U(\alpha)}{T}\int_0^T\int_{-h_0}^{\eta^c}\phi_x^c\,dydt \\ &= \overline{\int_{-h}^{\eta}u\,dy} - U(\alpha)\overline{\int_{-h_0}^{\eta^c}u^c\,dy} = 0\ ;\ U(\alpha) = \begin{cases} 0, \alpha \neq 0 \\ 1, \alpha = 0 \end{cases}. \end{aligned} \tag{8}$$

Both the superscript c and the sub script 0 express the physical quantity at infinite depth. Because of the nonlinear effect, waves over constant depth induce a net flux of water. In Equation (8), a deep-water streaming term is introduced that is adjusted by a unit function $U(\alpha)$ to ensure that it can be reduced to the deep-water condition when the bottom slope is equal to zero.

For a gentle bottom slope α, Equations (2) to (8) can be solved order by order in the following section.

III. ASYMPTOTIC SOLUTIONS

In this section, an explicit expression for the velocity potential of the wave field is first derived as a function of the bottom slope α and of the wave steepness ε to the third order in an Eulerian coordinate system. Then, the wave profile and the velocity components are transformed into a Lagrangian system. Finally, in the next section, the kinematic stability parameter is introduced and theoretical breaking-wave characteristics derived. The detailed computation is as follows:

First, the Laplace equation, Equation (2), and the corresponding boundary conditions, Equation (3) to (8), are used to obtain the asymptotic solutions. This study assumes that the relevant physical quantities can be expanded as a double power series of the parameter ε and the bottom slope α. Thus, the velocity potential ϕ, the free-surface displacement η, the wave number k, and the angular frequency σ can be obtained as follows:

$$\sigma = \sum_{\beta=0}^{\infty} \varepsilon^{\beta} \sigma_{\beta}(\lambda_0, a_0) = constant \tag{9}$$

$$k = \sum_{r=0}^{\infty} \sum_{l=0}^{\infty} \varepsilon^{r} \alpha^{l} k_{r,l}(k_{0,0}, k_{0,0}h; \lambda_0, a_0) \tag{10}$$

$$\begin{aligned} \eta &= \sum_{m=1}^{\infty} \varepsilon^{m} \eta_{m}(\lambda h, S; \alpha, \lambda_0, a_0) \\ &= \sum_{m=1}^{\infty} \sum_{n=0}^{\infty} \varepsilon^{m} \alpha^{n} \eta_{m,n}(\lambda h, S; \lambda_0, a_0) \\ &= \sum_{m=1}^{\infty} \sum_{n=0}^{\infty} \sum_{i=0}^{m} \varepsilon^{m} \alpha^{n} \eta_{m,n,i}(\lambda h, S; \lambda_0, a_0) \end{aligned} \tag{11}$$

$$\begin{aligned} \phi &= \sum_{m=1}^{\infty} \sum_{n=0}^{\infty} \varepsilon^{m} \alpha^{n} (\phi'_{m,n} + \phi_{m,n}) \\ &= \sum_{m=1}^{\infty} \sum_{n=0}^{\infty} \varepsilon^{m} \alpha^{n} \{\phi'_{m,n}(t, \sigma_0, a_0) \\ &+ \sum_{i=0}^{m} A_{m,n,i}(\lambda h, \lambda y, \lambda; \sigma_0, a_0)\, F_{m,n,i}(S) \times E_{m}(\lambda h, \lambda; \alpha) \\ &+ \int_{x_0}^{x} M_{m,n,0}(\lambda h, \lambda; \sigma_0, a_0)\, dx'\} \\ S &= \int_{x_0}^{x} k\, dx' - \sigma t \; ; \; E_{m}(\lambda h, \lambda, \alpha) \\ &= \exp[m \sum_{j=2}^{\infty} \alpha^{j} \int_{x_0}^{x} e_{j}(\lambda h, \lambda)\, dx'] \\ &= E_{m}; \; \lambda = k, \end{aligned} \tag{12}$$

where S is the phase function, x_0 denotes the x value at infinite depth, e_j is the wave amplitude influence factor, and $M_{m,n,0}$ is the return flow. The bottom slope α is assumed to be small; thus, the qth differentiations of $k_{r,l}$, $A_{m,n,i}$, and $M_{m,n,0}$ with respect to x are of order α^q:

$$\left(\frac{d^{q} k_{r,l}}{dx^{q}}, \frac{d^{q} e_{j}}{dx^{q}}, \frac{\partial^{q} A_{m,n,i}}{\partial x^{q}}, \frac{d^{q} M_{m,n,0}}{dx^{q}}\right) = O(\alpha^{q}) \tag{13}$$

Substituting Equations (9) to (13) into the governing equation and the boundary conditions (2) to (8), using the Taylor series expansion of functions at $y = 0$ instead of $y = \eta$, and collecting terms of the same order of ε and α yields the required equations to each order of approximation. Then different orders of $\varepsilon(m)$, $\alpha(n)$, and harmonic (i) may be separated, yielding a set of partial differential equations for each index (m, n, i). The boundary-value problems can be solved sequentially for orders of *m*, *n*, and *i*. The solution is as follows, where the notation shown is used for convenience:

$$\cosh = \mathrm{ch}, \sinh = \mathrm{sh}, \tanh = \mathrm{th}; \; I = \coth \lambda h \tag{14}$$

The solutions are obtained as follows:

For $O(\varepsilon^2\ \alpha)$, the solution for velocity potential function ϕ and the corresponding free-surface displacement η can be obtained from the boundary-value problem with corresponding order terms. The results are

$$\begin{aligned} \phi &= \sum_{m=1}^{\infty} \sum_{n=0}^{\infty} \varepsilon^{m} \alpha^{n} (\phi'_{m,n} + \phi_{m,n}) \\ &= [(A_{1,0,1} + \alpha^2 A_{1,2,1}) \sin S + (\alpha A_{1,1,1} + \alpha^3 A_{1,3,1}) \cos S] \\ &+ [A_{2,0,2} \sin 2S + \alpha (A_{2,1,2} \cos 2S + A_{2,1,0})\ ] \\ &+ [\phi'_{2,0} + \int_{x_0}^{x} M_{2,0,0}\, dx'] \end{aligned} \tag{15}$$

$$\begin{aligned} \eta &= \sum_{m=1}^{\infty} \sum_{n=0}^{\infty} \varepsilon^{m} \alpha^{n} \eta_{m,n} \\ &= [(\alpha a_{1,1,1} + \alpha^3 a_{1,3,1}) \sin S + (a + \ \alpha^2 a_{1,2,1}) \cos S] \\ &+ [\alpha a_{2,1,2} \sin 2S + a_{2,0,2} \cos 2S] + \eta_{2,0,0} \end{aligned} \tag{16}$$

$$\sigma = \sigma_0; \; k = k_0 + \alpha^2 k_{0,2}, \tag{17}$$

where

$$A_{1,0,1} = \frac{ag}{\sigma_0} \frac{\mathrm{ch}\lambda(h+y)}{\mathrm{ch}\lambda h};$$

$$a_{1,1,1} = a\left(\frac{\lambda^2 h^2}{D \mathrm{sh} 2\lambda h} - \lambda h + \frac{I^2}{D^2} \lambda h\right)$$

$$A_{1,1,1}=\frac{ag}{\sigma_0}\{[-\frac{\lambda^2(h+y)^2}{D\mathrm{sh}2\lambda h}+\lambda(h+y)]\times\frac{\mathrm{ch}\lambda(h+y)}{\mathrm{ch}\lambda h}-\frac{\lambda(h+y)}{D^2\,\mathrm{th}\lambda h}\frac{\mathrm{sh}\lambda(h+y)}{\mathrm{ch}\lambda h}\}$$

$$A_{1,2,1}=\frac{ag}{\sigma_0}\{[-\frac{\lambda^4(h+y)^4}{2(D\mathrm{sh}2\lambda h)^2}+\frac{\lambda^3(h+y)^3}{D\mathrm{sh}2\lambda h}-\frac{(D^4-4D+5I^2)}{2D^4}\lambda^2(h+y)^2+\frac{I\lambda(h+y)}{D^2}]\times\frac{\mathrm{ch}\lambda(h+y)}{\mathrm{ch}\lambda h}+[-\frac{4D+10\mathrm{ch}^2\lambda h}{3D^3\mathrm{sh}^2 2\lambda h}\lambda^3(h+y)^3+\frac{2(D+\mathrm{ch}^2\lambda h)}{D^2\mathrm{sh}2\lambda h}\lambda^2(h+y)^2-(\lambda-k_{0,2})(h+y)]\times\frac{\mathrm{sh}\lambda(h+y)}{\mathrm{ch}\lambda h}\}$$

$$a_{1,2,1}=a\{-\frac{(\lambda h)^4}{2(D\mathrm{sh}2\lambda h)^2}+\frac{(\lambda h)^3}{D\mathrm{sh}2\lambda h}-\frac{(4D+10\mathrm{ch}^2\lambda h)(\lambda h)^3}{3D^3 I\,\mathrm{sh}^2 2\lambda h}+[-\frac{D^4-4D+5I^2}{2D^4}+\frac{D+\mathrm{ch}^2\lambda h}{D^2\mathrm{ch}^2\lambda h}](\lambda h)^2+[\frac{I}{D^2}-(1-\frac{k_{0,2}}{\lambda})/I]\lambda h\}$$

$$k_{0,2}=[D^5+(D^4-18D^2+32D-15)\mathrm{ch}^2\lambda h+2D^2+(-3D^2+15D-15)I^2]\lambda/(3D^5)$$

$$a=a_0/\sqrt{D\mathrm{th}\lambda h}\ ;\ D=1+2\lambda h/\mathrm{sh}2\lambda h$$

$$A_{2,0,2}=[\frac{3}{8}\sigma_0 a^2\frac{\mathrm{ch}2\lambda(h+y)}{\mathrm{sh}^4\lambda h}];\ \phi'_{2,0}=-\sigma_0^2 a_0^2 t/(4\mathrm{sh}^2\lambda_0 h_0)$$

$$M_{2,0,0}=[\frac{-g\lambda^2 a^2}{2\sigma_0\lambda h}+U(\alpha)g\lambda\lambda_0 a_0^2/(2\sigma_0\lambda h)];\ \eta_{2,0,0}=\overline{\eta_{2,0}}=(\lambda_0 a_0^2/\mathrm{sh}2\lambda_0 h_0-\lambda a^2/\mathrm{sh}2\lambda h)/2\le 0$$

$$a_{2,0,2}=\frac{1}{4}\lambda a^2\frac{\mathrm{ch}\lambda h}{\mathrm{sh}^3\lambda h}(2\mathrm{sh}^2\lambda h+3)$$

$$a_{2,1,2}=\lambda a^2\{(3I^3-I)\lambda^2 h^2/(2D\mathrm{sh}2\lambda h)+[12DI^4+(-3D^2+6D+6)I^3-24DI^2+(D^2-5D-5)I+12D+(-D+1)I^{-1}]\lambda h/(2D^2)+[12D^2 I^7+(6D^2+3D)I^6+(-36D^2+24D)I^5+(-12D^2+D+22)I^4-12D^2 I^3+(-18D^2-3D+4)I^2+(36D^2-24D)I+(-8D^2-D+6)]/(8D^2)$$

$$A_{2,1,2}=\sigma_0 a^2\{[-\frac{3(I^4-1)\lambda^2(h+y)^2}{4D\mathrm{sh}2\lambda h}+\frac{3(I^2+1)\lambda(h+y)}{4\mathrm{sh}^2\lambda h}-(I^2+1)(12D^2I^6+(6D^2+3D)I^5-(48D^2-24D)I^4-(18D^2+2D-22)I^3+(36D^2-24D)I^2-(D+10)I)/(16D^2)]\frac{\mathrm{ch}2\lambda(h+y)}{\mathrm{ch}2\lambda h}-\frac{3[2D(I^4-1)+(D+1)(I^3+I)]}{4D^2\mathrm{sh}^2\lambda h}\lambda(h+y)\times\frac{\mathrm{sh}2\lambda(h+y)}{\mathrm{ch}2\lambda h}\}$$

$$A_{2,1,0}=\{\frac{\sigma_0}{4D}[\frac{Ia^2}{(\lambda h)^2}+\frac{2}{\lambda h}(\frac{D+1}{D}I^2-2)a^2]-U(\alpha)\frac{g\lambda_0 a_0^2}{4\sigma_0(\lambda h)^2}\}\times\lambda^2(h+y)^2+\{\frac{\sigma_0}{2D}[\frac{D-1}{\lambda h}I+\frac{1-2D}{D}\times(I^2-1)]a^2\frac{e^{\alpha\lambda(h+y)}-1}{e^{\alpha\lambda h}-1}-\sigma_0[\frac{Ia^2}{2\lambda h}-U(\alpha)\frac{\lambda_0 a_0^2 I}{2\lambda^2 h}]\}\times\lambda(h+y)+\{\frac{\sigma_0}{4D}[(\frac{4D-2}{D}I^2-2)a^2+(1+\frac{2}{D}-2D)\times\frac{Ia^2}{\lambda h}](\lambda h)-U(\alpha)\frac{g\lambda_0 a_0^2}{4\sigma_0}\}\frac{e^{\alpha\lambda(h+y)}-1}{e^{\alpha\lambda h}-1}$$

$$A_{1,3,1}=\frac{ag}{\sigma_0}\cdot\{\frac{\lambda^6(h+y)^6}{6D^3\sinh^3 2\lambda h}-\frac{\lambda^5(h+y)^5}{2D^2\sinh^2 2\lambda h}+[\frac{1}{2D\sinh 2\lambda h}+\frac{D(12D+40\cosh^2\lambda h-16D\sinh^2 2\lambda h+100\cosh^4\lambda h}{6D^5\sinh^3 2\lambda h}]\cdot\lambda^4(h+y)^4-[\frac{1}{6}+\frac{D(4D+10\cosh^2\lambda h)-2D\sinh^2 2\lambda h+10\cosh^4\lambda h}{D^4\sinh^2 2\lambda h}]\cdot\lambda^3(h+y)^3+[\frac{3D+(4-2k_{0,2}/\lambda)\mathrm{ch}^2\lambda h}{D^2\sinh 2\lambda h}-\frac{k_{0,2x}}{2\alpha^4\lambda^2}]\cdot\lambda^2(h+y)^2+(k_{0,2}-\lambda)(h+y)\}\times\frac{\cosh\lambda(h+y)}{\cosh\lambda h}+\frac{ag}{\sigma_0}\cdot\{\frac{20D+35\cosh^2\lambda h}{15D^4\sinh^3 2\lambda h}\cdot\lambda^5(h+y)^5-\frac{10D+10\cosh^2\lambda h}{3D^3\sinh^2 2\lambda h}\lambda^4\cdot(h+y)^4+[\frac{3D+\cosh^2\lambda h-k_{0,2}/\lambda\cdot D}{D^2\sinh 2\lambda h}+\frac{A_{xccc}}{6\alpha^3}]\cdot\lambda^3(h+y)^3-[\frac{D^4-4D+5\cosh^2\lambda h}{D^4}-\frac{k_{0,2}}{\lambda}]\cdot\lambda^2(h+y)^2+[\frac{2\cosh^2\lambda h}{D^2\sinh 2\lambda h}-e_3]\cdot\lambda(h+y)\}\cdot\frac{\sinh\lambda(h+y)}{\cosh\lambda h}$$

$$a_{1,3,1}=\frac{-\sigma}{g}\cdot\sum_{j=1}^{\infty}[M_{1,3,1,j}\cosh\lambda h+N_{1,3,1,j}\sinh\lambda h]\cdot h^j;$$

$$\sigma^2=g\lambda\tanh\lambda h=g\lambda_0\tanh\lambda_0 h.$$

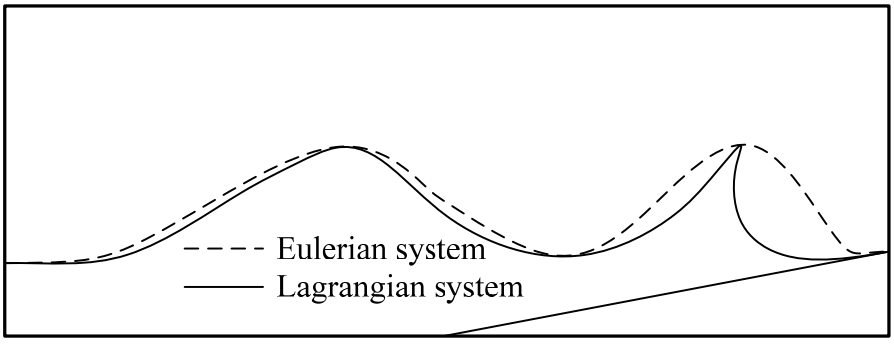

Fig. 2. Comparison of wave profiles with Lagrangian and Eulerian coordinates.

$$a = \frac{a_0}{(D\tanh\lambda h)^{1/2}};\ D = (1+\frac{2\lambda h}{\sinh 2\lambda h}), \qquad (18)$$

In Equations (15) to (18), $\sigma = \sigma_0 = 2\pi/T$ is the angular frequency, T is the wave period, and a_0 is the wave amplitude in deep water.

IV. BREAKING WAVES

1. Wave deformation

As a wave reaches its limit, the crest is fully developed as a summit and becomes highly asymmetrical. This asymmetric wave profile can be described by a Lagrangian coordinate system but cannot be captured by Eulerian solutions. Hence, the motion described in the Lagrangian system is close to that observed in reality (Chen et al., 2004).

The Eulerian and Lagrangian wave profile prior to breaking as a wave propagating over a gently sloping bottom ($0 < \alpha \le 1/10$) is illustrated in Fig. 2.

According to the velocity potential given in the previous section, the horizontal and vertical Eulerian velocity components, $u_e = \partial\phi/\partial x$ and $v_e = \partial\phi/\partial y$, of a fluid particle can be derived. As a wave shoals, the wave form becomes asymmetric, and the particle motion can be obtained by the transformation between Eulerian and Lagrangian coordinates. The Lagrangian velocity may be estimated from the Eulerian velocity (Chen et al., 2006) $\vec{V}_L(\vec{a},t) = \vec{V}_E[a\int_{t_0}^{t}\vec{V}_L(\vec{a},t') = \vec{V}_E(\vec{a},t) + \int_{t_0}^{t}\vec{V}_L(\vec{a},t')dt' \cdot \nabla_{\vec{a}}\vec{V}_E(\vec{a},t) + H.O.T.$

The Eulerian (Lagrangian) velocity is $\vec{V}_E(\vec{a},t)=[u_e,v_e]$ ($\vec{V}_L(\vec{a},t)=[u_l,v_l]$), and $\vec{a}$ is the position of a fluid particle at time $t = t_0$. The Eulerian motions can then be transferred into the Lagrangian system according to the trajectory of the fluid particle. The corresponding velocity components u_l and v_l are

$$\begin{aligned} u_l = u_e + (\int^t u_e dt)\frac{\partial u_e}{\partial x} + (\int^t v_e dt)\frac{\partial u_e}{\partial y} &= \sigma_0 a[(\alpha C_1 + \alpha^3 C_3)\frac{ch\lambda(h+y)}{sh\lambda h} + (\alpha S_1 + \alpha^3 S_3)\times\frac{sh\lambda(h+y)}{sh\lambda h}]\sin S \\ +\sigma_0 a[(1-\alpha^2 C_2)\frac{ch\lambda(h+y)}{sh\lambda h} - (\alpha^2 S_2)\frac{sh\lambda(h+y)}{sh\lambda h}]\cos S + 2\alpha\lambda\sigma_0 a^2[C_3\frac{ch2\lambda(h+y)}{ch2\lambda h} + S_3\frac{sh2\lambda(h+y)}{ch2\lambda h} & \\ -(C_1 + \frac{D+ch^2\lambda h}{D^2 sh2\lambda h})\frac{1}{sh^2\lambda h}]\sin 2S + \lambda\sigma_0 a^2(\frac{3}{4}\frac{ch2\lambda(h+y)}{sh^4\lambda h} - \frac{1}{2}\frac{1}{sh^2\lambda h})\cos 2S + [M_{2,0,0} + \frac{1}{2}\sigma_0\lambda a^2\frac{ch2\lambda(h+y)}{sh^2\lambda h}] & \end{aligned}, \qquad (19)$$

$$\begin{aligned} v_l = v_e + (\int^t u_e dt)\frac{\partial v_e}{\partial x} + (\int^t v_e dt)\frac{\partial v_e}{\partial y} &= \sigma_0 a[(1-\alpha^2 C_2)\frac{sh\lambda(h+y)}{sh\lambda h} - (\alpha^2 S_2)\frac{ch\lambda(h+y)}{sh\lambda h}]\sin S + \sigma_0 a[-(\alpha C_1 + \alpha^3 C_3)\frac{sh\lambda(h+y)}{sh\lambda h} \\ -(\alpha S_1 + \alpha^3 S_3)\frac{ch\lambda(h+y)}{sh\lambda h}]\cos S + \frac{3}{4}\lambda\sigma_0 a^2\frac{sh2\lambda(h+y)}{sh^4\lambda h}\times\sin 2S - 2\alpha\lambda\sigma_0 a^2[C_3\frac{sh2\lambda(h+y)}{ch2\lambda h} + S_3\frac{ch2\lambda(h+y)}{ch2\lambda h} & \\ -(\frac{\lambda(h+y)}{2Dsh2\lambda h} - \frac{1}{2})\frac{1}{sh^2\lambda h}]\cos 2S & \end{aligned}, \qquad (20)$$

Then, the displacement components X and Y of the fluid particle with initial average position (x,y) are obtained by direct integration as

$$\begin{aligned}
X &= \int^t u_l\,dt \\
&= a\{[(-1+\alpha^2 C_2)\sin S + (\alpha C_1 + \alpha^3 C_3)\cos S]\frac{\mathrm{ch}\lambda(h+y)}{\mathrm{sh}\lambda h} \\
&\quad + [\alpha^2 S_2 \sin S + (\alpha S_1 + \alpha^3 S_3)\cos S]\frac{\mathrm{sh}\lambda(h+y)}{\mathrm{sh}\lambda h}\} \\
&\quad - \frac{3}{8}\lambda a^2 \frac{ch2\lambda(h+y)}{sh^4\lambda h}\sin 2S + \frac{1}{4}\lambda a^2 \frac{1}{sh^2\lambda h}\sin 2S \\
&\quad + [M_{2,0,0} + \frac{1}{2}\sigma_0 \lambda a^2 \frac{ch2\lambda(h+y)}{sh^2\lambda h}]t + \alpha\lambda a^2[C_3 \frac{ch2\lambda(h+y)}{ch2\lambda h} \\
&\quad + S_3 \frac{sh2\lambda(h+y)}{ch2\lambda h} - (C_1 + \frac{D + ch^2\lambda h}{D^2 sh2\lambda h})\frac{1}{sh^2\lambda h}]\cos 2S
\end{aligned} \tag{21}$$

$$\begin{aligned}
Y &= \int^t v_l\,dt \\
&= a\{[-\alpha^2 S_2 \cos S + (\alpha S_1 + \alpha^3 S_3)\sin S]\frac{\mathrm{ch}\lambda(h+y)}{\mathrm{sh}\lambda h} \\
&\quad + [(1-\alpha^2 C_2)\cos S + (\alpha C_1 + \alpha^3 C_3)\sin S]\frac{\mathrm{sh}\lambda(h+y)}{\mathrm{sh}\lambda h}\}, \\
&\quad + \frac{3}{8}\lambda a^2 \frac{sh2\lambda(h+y)}{sh^4\lambda h}\cos 2S + \alpha\lambda a^2[C_3 \frac{sh2\lambda(h+y)}{ch2\lambda h} \\
&\quad + S_3 \frac{ch2\lambda(h+y)}{ch2\lambda h} - (\frac{\lambda(h+y)}{2Dsh2\lambda h} - \frac{1}{2})\frac{1}{sh^2\lambda h}]\sin 2S,
\end{aligned} \tag{22}$$

where

$$C_1 = \frac{\lambda^2(h+y)^2}{D\,\mathrm{sh}\,2\lambda h} - \lambda(h+y) + \frac{1}{D^2\,\mathrm{th}\,\lambda h};$$

$$S_1 = \frac{2(D + \mathrm{ch}^2\lambda h)}{D^2\,\mathrm{sh}\,2\lambda h}\lambda(h+y) - 1$$

$$\begin{aligned}
C_2 &= \frac{\lambda^4(h+y)^4}{2D^2\,\mathrm{sh}^2\,2\lambda h} - \frac{\lambda^3(h+y)^3}{D\,\mathrm{sh}\,2\lambda h} \\
&\quad + (\frac{1}{2} + \frac{4D^2 + 10D\,\mathrm{ch}^2\lambda h - 2D\,\mathrm{sh}^2\,2\lambda h + 10\,\mathrm{ch}^4\lambda h}{D^4\,\mathrm{sh}^2\,2\lambda h}) \\
&\quad \times \lambda^2(h+y)^2 + \frac{4D + 6\,\mathrm{ch}^2\lambda h}{D^2\,\mathrm{sh}\,2\lambda h}\lambda(h+y) - 1 + \frac{k_{0,2}}{\lambda}
\end{aligned}$$

$$\begin{aligned}
S_2 &= \frac{10(D + \mathrm{ch}^2\lambda h)}{3D^3\,\mathrm{sh}^2\,2\lambda h}\lambda^3(h+y)^3 \\
&\quad - \frac{5D + 2\,\mathrm{ch}^2\lambda h}{D^2\,\mathrm{sh}\,2\lambda h}\lambda^2(h+y)^2 \\
&\quad + (2 + \frac{5I^2 - 4D}{D^4} - \frac{k_{0,2}}{\lambda})\lambda(h+y) - \frac{I}{D^2}
\end{aligned}$$

$$\begin{aligned}
C_3 &= \frac{3(I^4-1)}{4Dsh2\lambda h}\lambda^2(h+y)^2 - \frac{3(I^2+1)}{4sh^2\lambda h}\lambda(h+y) \\
&\quad + \frac{1}{16D^2}(I^2+1)\times[12D^2I^6 + (6D^2+3D)I^5 \\
&\quad - (48D^2 - 24D)I^4 \quad - (18D^2 + 2D - 22)I^3 \\
&\quad + (36D^2 - 24D)I^2 - (D+10)I] \\
&\quad + \frac{3[2D(I^4-1) + (D+1)(I^3+I)]}{4Dsh^2\lambda h}
\end{aligned}$$

$$S_3 = \frac{3[2D(I^4-1) + (D+1)(I^3+I)]}{4D^2 sh^2\lambda h} + \frac{3(I^4-1)}{4Dsh2\lambda h}$$

Substituting y = 0 into Equations (21) and (22), the displacement of a water particle on the free surface ξ (x-direction) and ς (y-direction) can be given as

$$\begin{aligned}
\xi &= x + (X)_{y=0} \\
&= x + a\{[(-1+\alpha^2 C_{20})\sin S + (\alpha C_{10} + \alpha^3 C_{30})\cos S]I \\
&\quad + [\alpha^2 S_{20}\sin S + (\alpha S_{10} + \alpha^3 S_{30})\cos S]\} \\
&\quad - \frac{3}{8}\lambda a^2 \frac{ch2\lambda h}{sh^4\lambda h}\times\sin 2S + \frac{1}{4}\lambda a^2 \frac{1}{sh^2\lambda h}\sin 2S + [M_{2,0,0} \\
&\quad + \frac{1}{2}\sigma_0 \lambda a^2 \frac{ch2\lambda h}{sh^2\lambda h}]t + \alpha\lambda a^2[C_{30} + S_{30} th2\lambda h \\
&\quad - (C_{10} + \frac{D + ch^2\lambda h}{D^2 sh2\lambda h})\frac{1}{sh^2\lambda h}]\cos 2S,
\end{aligned} \tag{23}$$

$$\begin{aligned}
\varsigma &= (Y)_{y=0} \\
&= a\{[-\alpha^2 S_{20}\cos S + (\alpha S_{10} + \alpha^3 S_{30})\sin S]I \\
&\quad + [(1-\alpha^2 C_{20})\cos S + (\alpha C_{10} + \alpha^3 C_{30})\sin S]\}, \\
&\quad + \frac{3}{8}\lambda a^2 \frac{sh2\lambda h}{sh^4\lambda h}\cos 2S + \alpha\lambda a^2[C_{30} th2\lambda h + S_{30} \\
&\quad - (\frac{\lambda h}{2Dsh2\lambda h} - \frac{1}{2})\frac{1}{sh^2\lambda h}]\sin 2S,
\end{aligned} \tag{24}$$

where (ξ,ς) is the position of the fluid particle on the free surface (y = 0).

In the above expressions, C_{10}, S_{10}, C_{20}, S_{20}, C_{30}, and S_{30} are deduced from C_1, S_1, C_2, S_2, C_3, and S_3 given in Equations (23) and (24), with the substitution y = 0, where the subscript 0 represents the free surface.

2. Breaker characteristics

The increase in wave height owing to the shoaling effect becomes depth-limited as the wave propagates into shallow waters. The celerity is reduced; the particle velocity of the wave crest is faster than the wave celerity, and the wave breaks. To describe the breaking-wave mechanism, the kinematic stability parameter $(K.S.P.)$ is applied, and the breaking-wave

criterion is

$$K.S.P.=\frac{u_{0b}}{C}=1, \tag{25}$$

where C is wave celerity and u_{0b} is the horizontal velocity of the particle at the wave crest.

In accordance with Equation (18), the breaking amplitude parameters a_b may be written as

$$a_b=\frac{a_0}{(D_b\tanh k_b h_b)^{1/2}} \tag{26}$$

where $D_b=(1+\frac{2k_bh_b}{\sinh 2k_bh_b})$, and the subscript b denotes the breaking condition.

Up to the breaking point, the linear dispersion relation is still valid, and hence

$$\sigma^2=gk_b\tanh k_bh_b;\ \sigma=k_bC_b;\ L_b=2\pi/k_b. \tag{27}$$

where L_b is the wavelength, k_b is the wave number, C_b is the celerity of the breaking wave, and h_b is the breaking-wave depth, respectively.

The Lagrangian horizontal velocities u_l evaluated at y = 0 can be simplified as

$$\begin{aligned}(u_l)_0=&\sigma_0 a[(\alpha C_{10}+\alpha^3C_{30})I+(\alpha S_{10}+\alpha^3S_{30})]\sin S\\&+\sigma_0 a\,[(1-\alpha^2C_{20})I-(\alpha^2S_{20})]\cos S\\&+2\alpha\lambda\sigma_0a^2[C_{30}+S_{30}\,th2\lambda h-(C_{10}+\frac{D+ch^2\lambda h}{D^2sh2\lambda h})\\&\times\frac{1}{sh^2\lambda h}]\sin 2S+\lambda\sigma_0a^2(\frac{3}{4}\frac{ch2\lambda h}{sh^4\lambda h}-\frac{1}{2}\frac{1}{sh^2\lambda h})\cos 2S\\&+[M_{2,0,0}+\frac{1}{2}\sigma_0\lambda a^2\frac{ch2\lambda h}{sh^2\lambda h}],\end{aligned} \tag{28}$$

The breaker condition is defined by taking the extreme value of the horizontal velocity

$$\frac{\partial(u_l)_0}{\partial t}=0 \tag{29}$$

The phase angle of the breaking wave S_b can be solved, and this condition also implies that the water surface elevation ς has an extreme value.

The resulting Lagrangian horizontal velocity of the breaking wave on the free surface, based on Eq. (28), is denoted as $(u_l)_{0b}$:

$$\begin{aligned}(u_l)_{0b}=&\sigma_0a_b[(\alpha C_{10b}+\alpha^3C_{30b})\coth k_bh_b\\&+(\alpha S_{10b}+\alpha^3S_{30b})]\sin S_b+\sigma_0a_b[(1-\alpha^2C_{20b})\coth k_bh_b\\&-(\alpha^2S_{20b})]\cos S_b+2\alpha k_b\sigma_0{a_b}^2[C_{30b}+S_{30b}th2k_bh_b\\&-(C_{10b}+\frac{D_b+ch^2k_bh_b}{{D_b}^2sh2k_bh_b})\frac{1}{sh^2k_bh_b}]\sin 2S_b\\&+k_b\sigma_0{a_b}^2\times(\frac{3}{4}\frac{ch2k_bh_b}{sh^4k_bh_b}-\frac{1}{2}\frac{1}{sh^2k_bh_b})\cos 2S_b\\&+[\frac{-\sigma_0{a_b}^2}{2thk_bh_b}+\frac{1}{2}\sigma_0k_b{a_b}^2\frac{ch2k_bh_b}{sh^2k_bh_b}].\end{aligned} \tag{30}$$

C_{10b}, C_{20b}, C_{30b}, S_{10b}, S_{20b}, S_{30b}, and k_b are deduced from C_{10}, C_{20}, C_{30}, S_{10}, S_{20}, S_{30}, and k, with the substitution $a = a_b$, $D = D_b$, $k = k_b$, and $h = h_b$, where the subscript b represents the breaking wave.

Thus, the breaking-wave criterion can be rewritten in the more specific form

$$K.S.P.=\frac{(u_l)_{0b}}{C_b}=1. \tag{31}$$

This criterion, after substituting the previous Lagrangian velocity, becomes

$$\begin{aligned}&k_ba_b[(\alpha C_{10b}+\alpha^3C_{30b})\coth k_bh_b+(\alpha S_{10b}+\alpha^3S_{30b})]\sin S_b\\&+k_ba_b[(1-\alpha^2C_{20b})\coth k_bh_b\\&-(\alpha^2S_{20b})]\cos S_b+2\alpha\times{k_b}^2{a_b}^2[C_{30b}+S_{30b}th2k_bh_b\\&-(C_{10b}+\frac{D_b+ch^2k_bh_b}{{D_b}^2sh2k_bh_b})\times\frac{1}{sh^2k_bh_b}]\sin 2S_b\\&+{k_b}^2{a_b}^2(\frac{3}{4}\frac{ch2k_bh_b}{sh^4k_bh_b}-\frac{1}{2}\frac{1}{sh^2k_bh_b})\times\cos 2S_b\\&+[\frac{-k_b{a_b}^2}{2thk_bh_b}+\frac{1}{2}{k_b}^2{a_b}^2\frac{ch2k_bh_b}{sh^2k_bh_b}]=1.\end{aligned} \tag{32}$$

By utilizing Equations (27), (29), and (32), we can solve h_b, k_b, and S_b. The maximum surface elevation $\varsigma_{\max}$, which appears when a wave breaks, is given by

$$\begin{aligned}\varsigma_{\max}=&a_b\{[(1-\alpha^2C_{20b}-\alpha^2S_{20b}\coth k_bh_b)\cos S_b\\&+[(\alpha C_{10b}+\alpha^3C_{30b})+(\alpha S_{10b}+\alpha^3S_{30b})\\&\times\coth k_bh_b]\sin S_b\}+\frac{3}{8}k_b{a_b}^2\times\frac{sh2k_bh_b}{sh^4k_bh_b}\cos 2S_b\\&+\alpha k_b{a_b}^2[C_{30b}th2k_bh_b+S_{30b}\\&-(\frac{k_bh_b}{2D_bsh2k_bh_b}-\frac{1}{2})\frac{1}{sh^2k_bh_b}]\sin 2S_b.\end{aligned} \tag{33}$$

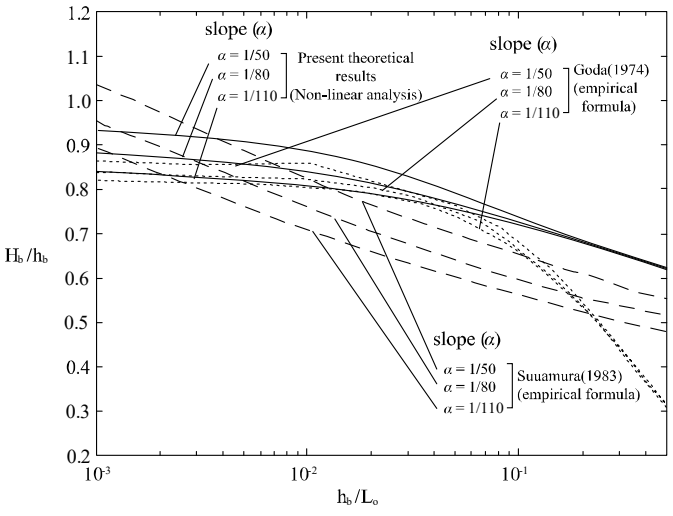

Fig. 3. Relationship between H_b/h_b and h_b/L_0

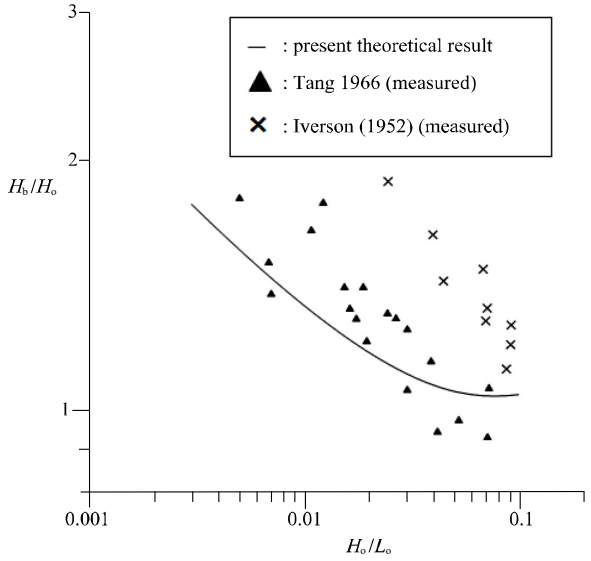

Fig. 4. Relationship between H_b/H_0 and H_0/L_0 for $\alpha = 1/20$.

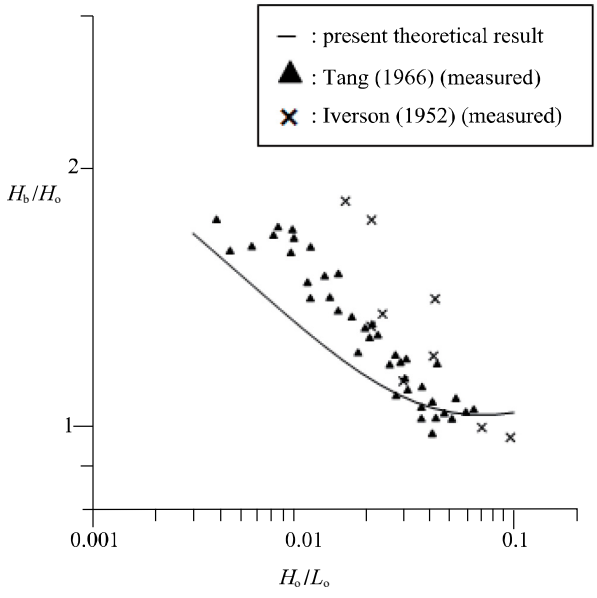

Fig. 5. Relationship between H_b/H_0 and H_0/L_0 for $\alpha = 1/50$.

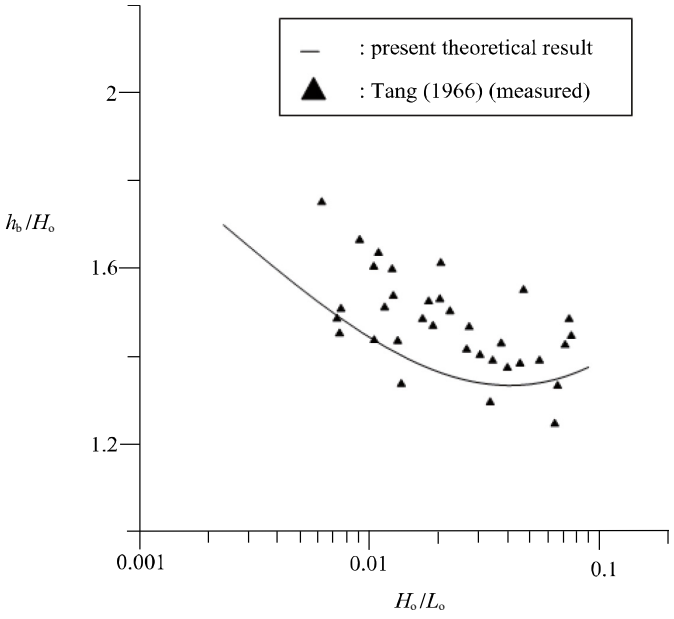

Fig. 6. Relationship between h_b/H_0 and H_0/L_0 for $\alpha = 1/20$.

Similarly, we can solve the minimum elevation of breaking-wave depth $\varsigma_{\min}$, and the breaking-wave height H_b is then derived as

$$H_b = (\varsigma_{\max} - \varsigma_{\min}) = (\varsigma_b - \varsigma_{\min}) \tag{34}$$

where $\varsigma_b = \varsigma_{\max}$.

V. THEORY VALIDATION AND DISCUSSION

Many factors influence wave breaking, including wave steepness, wave height, and bottom slope. The breaking phenomenon is so complicated that most related studies have described breaking-wave characteristics only from experimental studies and empirical or semiempirical formulae calibrated from laboratory data. However, this paper presents a theoretical investigation of nonlinear surface-wave propagation over a sloping bottom and compares the results of the present theory with previously published results (Fig. 3 to Fig. 8).

Fig. 3 to Fig. 5 demonstrate that H_b/h_b decreases as h_b/L_0 increases and that H_b/H_0 decreases as H_0/L_0 increases. Fig.

3 shows that the present analytical solutions follow the same trend that other research results do. Fig. 4 to Fig. 8 also demonstrate that the theoretical modeling results follow the same trend that experimental measurements in other studies have.

VI. CONCLUSIONS

This paper provides an analytical solution for breaker characteristics. The solution has not been appropriately addressed in other studies. The present theoretical solutions are compared with the results of other scholars, as shown in Fig. 3 to Fig. 5. They also show that the present analytical solutions follow the same trend that previously published results have. The main outcomes of this study are as follows:

1. This paper provides a theoretical solution for a wave propagating over a uniformly sloping bottom, from deep water to shallow water, until the wave breaks. The theoretical results of this study reveal characteristics of breaking waves that have not been described in other studies.
2. The respective theoretical modeling requires only knowledge of the incident wave conditions and of the bottom slope for breaking-wave characteristics to be obtained.

REFERENCES

Biesel, F. (1952). Study of propagation in water of gradually varying depth. U.S. National Bureau of Standards, Gravity Waves, NBS Circular 521, 243-253.

Chang, H. K. (1999). Shoaling of nonlinear waves over a gently sloping bottom. Journal of the Chinese institute of civil and hydraulic Engineering 11 (1), 175-180.

Chanson, H. and J.-F. Lee (1997). Plunging jet characteristics of plunging breakers. Coastal Engineering 31, 125-141.

Chen, Y. Y. and L.W. Tang (1992). Surface-wave propagation on gentle sloping bottom. Proc. of the 14th Ocean Engineering Conf. in Taiwan, 1-22. (in Chinese)

Chen, Y. Y., B. D. Yang, L. W. Tang, S. H. Ou and R. C. John Hsu (2004). Transformation of progressive waves propagating obliquely on a gentle slope. Journal of Waterway, Port, Coastal and Ocean Engineering 130 (4, 162-169.

Chen, Y. Y., H.C. Hsu, G. Y. Chen and H. H. Hwung (2006). Theoretical Analysis for Surface Waves Propagation on Sloping Bottoms, Part 2. Wave Motion 43, 339-356.

Chen, Y. Y., H.H. Hwung and H. C. Hsu (2005). Theoretical Analysis of Surface Waves Propagation on Sloping Bottoms, Part 1. Wave Motion Vol. 42, 335-351.

Deo, M. C. and S. S. Jagdale (2003). Prediction of breaking waves with neural networks. Ocean Engineering 30 (9), 1163-1178.

Elgar, S. and R.T. Guza (1985). Shoaling gravity waves: comparisons between field observations Linear theory and a nonlinear model. Journal of Fluid Mechanics 158, 47-70.

Galvin, C. J. (1968). Breaker type classifications of three laboratory beaches. J. Geophys Res. 73 (12), 3651-3659.

Goda, Y. (1970). A synthesis of breaker indices. Trans. Japan Soc. Civil Engrs. 2, Part 2, 227-230.

Goda, Y. (2004). A 2-D random wave transformation model with gradational breaker index. Coastal Engineering Journal 46 (1), 1-38.

Gotoh, H. and T. Sakai (1999). Lagrangian simulation of breaking waves using particle method. Coastal Engineering Journal 41, 303-326.

Hansen, J. B. (1990). Periodic waves in the surf zone: Analysis of experimental data. Coastal Eng. 14 (1), 19-41.

Hsiao, S. C., T. W. Hsu,, T. C. Lin,, and Y. H. Chang, (2008). On the evolution and run-up of breaking solitary waves on a mild sloping beach. Coastal Engineering 55, 975-988.

Hsieh, C. M., R. R. Hwang, M. J. Chern and W. C. Yang (2008). Using RANS to simulate breaking wave on a slopping bed. Proceedings of 18th International Offshore (Ocean) and Polar Engineering Conference, 684-690.

Hsieh, C. M., R. R. Hwang, Y. F. Peng, W. C. Yang and M. J. Chern (2007). Numerical simulations of solitary wave running and breaking on a slopping bed. Proceedings of 17th International Offshore (Ocean) and Polar Engineering Conference, 2321-2326.

Hsu, H.C., Y.Y. Chen,, and H.H. Hwung, (2001). Surface wave propagation on a gentle sloping bottom. Proc. of the 23rd Ocean Engineering Conf. in Taiwan, 33-40. (in Chinese)

Iwagaki, Y., T. Sakai, K. Tsukioka and N. Sawai (1974). Relationship between vertical distribution of water particle velocity and type of breakers on beaches. Coastal Eng. in Japan 17, 51-58.

Keller, J. B. (1958). Surface waves on water of non-uniform depth. J. Fluid Mech. 4, 607-614 .

L'e M'ehaut'e, B. and R.C.Y. Koh (1967). On the breaking of waves arriving at an angle to the shore. J. Hydraul. Res. 5 (1), 67-88.

Li, M. S., Y. Y. Chen and H. H. Hsu (2013). A. Torres-Freyermuth, Experiment and Lagrangian modeling of nonlinear water waves propagation on a sloping bottom. Ocean Engineering 64, 36-48.

Ogawa, Y. and N. Shuto (1984). Run-up of periodic waves on beaches of non-uniform slope. Proc. 19th Coastal Eng. Conf., ASCE, 328-334.

Rattanapitikon, W. and T. Shibayama (2000). Verification and modification of breaker height formulas. Coastal Engineering Journal 42 (4), 389-406.

Saeki, H. S. A. O. Hanayasu and K. Takgi (1971). The shoaling and run-up height of the solitary wave. Coastal Engineering in Japan 14, 25-42.

Seyama, A. and A. Kimura (1988). The measured properties of irregular wave breaking and wave height change after breaking on slope. Proc. 21st Coastal Eng. ASCE, 419-432.

Street, R. L. and F. E. Camfield (1966). Observations and experiments on solitary wave deformation. Proc. 10th Conf. Coastal Eng., 284-301.

Sunamura, T. (1980). A laboratory study of offshore transport of sediment and a model for eroding beaches. Proc. 17th Coastal Eng. Conf., ASCE, 1051-1070.

Sunamura, T. (1983). Determination of breaker height and depth in the field. Ann. Rep., Inst. Geosci., Univ. Tsukuba (8), 53-54.

Sunamura, T. and K. Horikawa (1974). Two-dimensional beach transformation due to waves. Proc. 14th Coastal Eng. Conf., ASCE, 920-938.

Tang, L.W. (1966). Coastal engineering researches on the western coast of Taiwan. Proc. 10th Conference on coastal Engineering, 1275-1290.

Ting, C.-L., M.-C. Lin, W.-C. Hu and Y.-H. Hsieh (2002). Reformed wave characteristics of waves breaking on a steep-sloped step. Proceedings of the 24th Ocean Engineering Conference in Taiwan, 51-56. (in Chinese)

Tsai, C. P., H. B. Chen, H.H. Hwung and M. J. Huang (2005). Examination of empirical formulas for wave shoaling and breaking on steep slopes. Ocean Engineering 32, 469-483.

.